



HAL
open science

H3K9me2 genome-wide distribution in the holocentric insect *Spodoptera frugiperda* (Lepidoptera: Noctuidae)

Sandra Nhim, Sylvie Gimenez, Rima Nait-Saidi, Dany Severac, Kiwoong Nam, Emmanuelle d'Alençon, Nicolas Nègre

► **To cite this version:**

Sandra Nhim, Sylvie Gimenez, Rima Nait-Saidi, Dany Severac, Kiwoong Nam, et al.. H3K9me2 genome-wide distribution in the holocentric insect *Spodoptera frugiperda* (Lepidoptera: Noctuidae). *Genomics*, 2022, 114 (1), pp.384 - 397. 10.1016/j.ygeno.2021.12.014 . hal-03574469

HAL Id: hal-03574469

<https://hal.inrae.fr/hal-03574469>

Submitted on 15 Feb 2022

HAL is a multi-disciplinary open access archive for the deposit and dissemination of scientific research documents, whether they are published or not. The documents may come from teaching and research institutions in France or abroad, or from public or private research centers.

L'archive ouverte pluridisciplinaire **HAL**, est destinée au dépôt et à la diffusion de documents scientifiques de niveau recherche, publiés ou non, émanant des établissements d'enseignement et de recherche français ou étrangers, des laboratoires publics ou privés.



Distributed under a Creative Commons Attribution - NonCommercial 4.0 International License



H3K9me2 genome-wide distribution in the holocentric insect *Spodoptera frugiperda* (Lepidoptera: Noctuidae)

Sandra Nhim^a, Sylvie Gimenez^a, Rima Nait-Saidi^a, Dany Severac^b, Kiwoong Nam^a,
Emmanuelle d'Alençon^a, Nicolas Nègre^{a,*}

^a DGIMI, Univ Montpellier, INRAE, Montpellier, France

^b MGX, Univ Montpellier, CNRS, INSERM, Montpellier, France

ARTICLE INFO

Keywords:

Heterochromatin
H3K9me2
Spodoptera frugiperda
Holocentrism
ChIP-Seq

ABSTRACT

Background: Eukaryotic genomes are packaged by Histone proteins in a structure called chromatin. There are different chromatin types. Euchromatin is typically associated with decondensed, transcriptionally active regions and heterochromatin to more condensed regions of the chromosomes. Methylation of Lysine 9 of Histone H3 (H3K9me) is a conserved biochemical marker of heterochromatin. In many organisms, heterochromatin is usually localized at telomeric as well as pericentromeric regions but can also be found at interstitial chromosomal loci. This distribution may vary in different species depending on their general chromosomal organization. Holocentric species such as *Spodoptera frugiperda* (Lepidoptera: Noctuidae) possess dispersed centromeres instead of a monocentric one and thus no observable pericentromeric compartment. To identify the localization of heterochromatin in such species we performed ChIP-Seq experiments and analyzed the distribution of the heterochromatin marker H3K9me2 in the Sf9 cell line and whole 4th instar larvae (L4) in relation to RNA-Seq data. **Results:** In both samples we measured an enrichment of H3K9me2 at the (sub) telomeres, rDNA loci, and satellite DNA sequences, which could represent dispersed centromeric regions. We also observed that density of H3K9me2 is positively correlated with transposable elements and protein-coding genes. But contrary to most model organisms, H3K9me2 density is not correlated with transcriptional repression.

Conclusion: This is the first genome-wide ChIP-Seq analysis conducted in *S. frugiperda* for H3K9me2. Compared to model organisms, this mark is found in expected chromosomal compartments such as rDNA and telomeres. However, it is also localized at numerous dispersed regions, instead of the well described large pericentromeric domains, indicating that H3K9me2 might not represent a classical heterochromatin marker in Lepidoptera. (242 words)

1. Introduction

The nuclear organization of the genome into chromatin is a hallmark of eukaryotes. DNA is wrapped around histone proteins to form nucleosomes that constitute basic units of chromatin [46]. Two chromatin types are classically described based on the compaction of nucleosomes along the genome. The euchromatin represents “open” and less compacted chromatin structures and is usually associated with active gene transcription. On the other hand, heterochromatin designates regions of the chromosomes that are more compact, with a higher nucleosome density [24]. Genes within heterochromatin are regarded to be transcriptionally repressed.

Several types of heterochromatin have been described. Constitutive

heterochromatin (c-Het), contrary to facultative heterochromatin, remains persistently compacted despite cell cycle and developmental stages, environmental states or even studied species [2,12,28]. It is usually located at important chromosomal features such as telomeres, rDNA loci and pericentromeric regions [68]. Those regions are usually gene poor and transcriptionally silenced [2,12]. Understood as a genomic safety guard from transposons [28], c-Het associated regions are often enriched in repeated sequences such as satellite DNA and transposable elements. The transcriptional silencing by c-Het is due to its compaction which is achieved by chemical modifications of histones. The classical marker of c-Het in all eukaryotes is the post translational methylation of the lysine 9 of Histone H3 (H3K9me) [26,34,44]. This methylation mark deposited by SET domain proteins such as Su(var)3–9

* Corresponding author.

E-mail address: nicolas.negre@umontpellier.fr (N. Nègre).

<https://doi.org/10.1016/j.ygeno.2021.12.014>

Received 9 July 2021; Received in revised form 2 November 2021; Accepted 15 December 2021

Available online 28 December 2021

0888-7543/© 2022 The Authors.

Published by Elsevier Inc.

This is an open access article under the CC BY-NC-ND license

(<http://creativecommons.org/licenses/by-nc-nd/4.0/>).

[67] and G9a ([84]; Makoto [36,85]) is recognized by chromo-domain containing proteins belonging to HP1s family [37,45,48,52]. HP1 proteins assemble as homodimers to form the ultrastructural 3D compaction detected by cytology [89]. This compaction impairs the binding of other DNA associated proteins such as transcription factors and RNA polymerases, which explains the repressive effect of heterochromatin. These properties of c-Het have been well described in model organisms, from yeast to mammals and thus are thought to be conserved.

With developments of sequencing, biochemical methods and growing interest for non-model organisms [86], the classical c-Het features are being reconsidered [23]. Underlying DNA sequences can show rapid turnover, a fact particularly true for centromeres [25]. Depending on cell cycle phases, nascent non coding RNAs from telomeres and pericentromeres contribute to the regulation of their biology [2,4]. H3K9me distribution has been shown to vary and dynamic apposition of histone marks has also been reported outside of primary c-Het regions [92] in heterochromatin “islands” [40,68]. In human and mouse, interstitial domains called LOCKS, spanning several Mb, dynamically switch to heterochromatin state, marked by Lysine 9 methylation, in specialized cells, supposedly to limit pluripotency [47,92]. Beside these controlled variations, c-Het can unpredictably change in terms of associated proteins or even DNA sequences. This causes several defects in development or represent molecular basis of hybrid incompatibilities between close species [11,17,27,31,72].

While most studies on c-Het have been performed on monocentric species, a particular case of c-Het dynamic is found in holocentric organisms. Their chromosomes have no cytological hypercompacted regions and possess dispersed centromeres instead of unique ones per chromosome [74]. Classical heterochromatin compartmentation and properties are thought to be absent. Holocentrism has been described in several plants, in some nematodes and some insect orders [14,93]. Phylogenetic analysis indicates that holocentric species might have derived several times from monocentric species by convergent evolution [16,51]. This is supported by different centromeric molecular signatures between holocentric species. In monocentric species, major 150 bp satellite forming centromeres are packaged in CenH3 rich nucleosomes that are encompassed by peripheral H3K9me2/3 regions [14,50]. But, except for the plant *Rhynchospora pubera* [49], described holocentric species have lost those centromeric repeated sequences. CenH3 is present in nematodes [18,81] and in plants [61,95] but has been lost in other holocentric insects [14]. A recent study proposed that in Lepidoptera, CenH3 function has been replaced by H3K27me3, a facultative heterochromatin mark [75]. More importantly H3K9me2 signal surrounding centromeres is thought to be lost in these organisms, unlike holocentric *C.elegans* [81]. Previous studies conducted on Lepidoptera showed nonetheless that H3K9me2 is still associated to repeated DNA at rDNA loci and sexual chromosomes [6,80].

In this paper, we aim to clarify H3K9me2 heterochromatin distribution in *S. frugiperda* (Lepidoptera: Noctuidae), a crop pest causing severe damages to plants at larval stage. Since the *S. frugiperda* distribution area has recently been extended from the American continent to a worldwide invasion [20], there is an urge to understand its adaptive potential when confronted with new ecosystems. In particular, chromatin properties could influence phenotypic plasticity in response to environmental conditions [19,78]. *S.frugiperda* constitutes also an emergent epigenetic model organism with published reference genomes for different strains and cell lines [22,32,56,57,96], histone modifications and non-coding RNAs being previously characterized [1,54,80] as well as a growing body of RNA-Seq data [62]. Another advantage lies in the well-established Sf9 cell line, derived from *S. frugiperda* ovarian tissues, providing non limiting material for biochemical assays [88]. We performed H3K9me2 ChIP-Seq and RNA-Seq on two different samples: Sf9 cell lines and whole 4th instar larvae (L4). In both samples, we confirmed the association of H3K9me2 at c-Het domains such as telomeres, rDNA locus and satellite sequences that might represent vestigial centromeres. We found a strong association of H3K9me2 with repeat

elements as well as gene bodies. And we show that H3K9me2 enrichment at these elements is not associated with transcriptional repression or activation, raising the question of its role in chromosomal organization in holocentric Lepidoptera.

2. Material and methods

2.1. *S. frugiperda* rearing and Sf9 cell line maintenance

L4 insects have been raised in controlled laboratory conditions of 16 h:8 h light/dark photoperiod cycle, ~40% mean hygrometry and ~24 °C temperature. The insects derived from pupae individuals collected in 2001 in Guadeloupe. This laboratory population corresponds to previously published reference genome assemblies [22,55].

Immortalized Sf9 cell line derived from *S. frugiperda* ovarian tissues [88]. The cell line was acquired from ATCC (<https://www.atcc.org/products/crl-1711>) and has been cultured following the manufacturer protocol recommendations.

2.2. Western blot

Chromatin extracts were prepared from Sf9 cells and L4 insects as described below for the ChIP procedure. Total proteins have been first quantified by colorimetric Bradford method and equivalent quantities were used for a 15% SDS/PAGE. After migration, proteins from the gel were transferred onto a PVDF membrane. The membrane was incubated overnight with mouse monoclonal H3K9me2 antibody (Abcam 1220) and revealed with an ECL kit.

2.3. Immunofluorescence on Sf9 cell lines

Sf9 cells were grown to confluence with standard Schneider medium, then scraped and collected in 50 mL Falcon tubes. Cells were then diluted up to 3.105 cells/ml and 1 mL was used for each immunostaining condition for 1 well of a 12-well plate. Plates with round glass coverslips and 1 mL of cell dilution were then placed at 28 °C for 4 h, allowing the cells to sediment on the coverslip. The culture medium was then removed, plates washed with 1× PBS and fixed with paraformaldehyde 4%, 20 min at room temperature. Coverslips were rinsed twice with PBS before processing with immunostaining.

For immunostaining, coverslips in the plates were permeabilized with 1 mL of PBS 1× + Triton 1% per well for 30 min at room temperature. The solution was removed, and the cells were blocked with PBS 1× + BSA 1% for 30 min at room temperature. The solution was removed and staining with the primary antibody (anti-H3K9m2, Abcam 1220) diluted in PBS-BSA 0.1% was performed. We used 1/100 and 1/220 dilutions (50 µL / well) and we kept a control non-treated well. Incubation was done 1 h at room temperature. Primary antibody was rinsed twice in PBS 1× before adding the secondary antibody (anti-mouse Alexa568) diluted 1/500 in PBS 1× – BSA 0.1% (~100 µL per well) 30–45 min at room temperature in the dark. Still in the dark, coverslips were rinsed once in PBS 1×, then incubated with DAPI (1 mg/mL diluted 1/1000 per condition) for 5 min and rinsed again. Coverslips were then mounted on a microscopy slide with 1 drop of ProLong Antifade Mountant (ThermoFischer Scientific) and after 30 min, sealed with transparent nail polish. Slides were kept in the dark at 4 °C until observation with an Apotome microscope (Zeiss).

2.4. ChIP-Seq and RNA-Seq

We performed ChIP-Seq following an adapted protocol by [58] on 4th instar whole larvae and Sf9 cell culture.

Briefly, biological samples are being crushed in a douncer, in presence of 1% formaldehyde and incubated for 15 min to allow protein-DNA crosslinking. Crosslinking was quenched by the addition of 2.5 mM glycine up to a final concentration of 225 mM. Chromatin was then

fragmented using a Bioruptor sonicator (Diagenode). A 250 μ L aliquot of sonicated chromatin at this stage is used as the Input sample.

For the immunoprecipitation, 250 μ L of sonicated chromatin is incubated for 4 h with 2.5 μ L of primary antibody (anti-H3K9me2, Abcam 1220) at 4 °C, then with 100 μ L of 50% Protein-A sepharose beads (CL4B) for again 4 h. Beads were then centrifuged and washed. Chromatin was eluted from the beads with a 50 mM Tris-HCl buffer with 1% SDS and 10 mM EDTA. To reverse the cross-linking, this immunoprecipitate was incubated overnight at 65 °C and then 2–3 h at 50 °C with proteinase K. DNA was purified from this precipitate with 500 μ L of phenol-chloroform and 55 μ L of 4 M LiCl. The DNA from the aqueous phase is precipitated with 100% ethanol and the pellet dried and resuspended in water. Chromatin was prepared from 50 L4 larvae pool and 50 mL of confluent cells per IP condition. Two biological replicates for input and ChIP conditions have been systematically produced except for larvae (1 Input see Table 1). DNA was used at this stage to produce Illumina libraries and sequencing in 50 bp single-end.

We also performed RNA-Seq experiments from Sf9 cell lines. RNA was purified using TRIzol (Invitrogen) following manufacturer's instructions and sent to Genewiz for strand-oriented, mRNA sequencing. Previously published RNA-Seq data for L4 [62] genomes were used to perform combined analysis.

Datasets are available in ArrayExpress (<https://www.ebi.ac.uk/arraxpress/>) with the following accession numbers: E-MTAB-6540 for L4 RNA-Seq; E-MATB-10686 for Sf9 RNA-Seq and E-MTAB-10721 for ChIP-Seq experiments.

2.5. H3K9me2 ChIP-Seq analysis

Raw reads from fastq files have been filtered using cutadapt software which trims remaining adapters, low quality (phredscore <35) and short length sequences (<40 nt). Corresponding samples alignments were performed using stringent parameters with Bowtie2 (--endtoend --very-sensitive, [38]) against Sf9 [57] and L4 genomes [55].

We next divided the genomes into bins of 50 bp so Deeptools software [66] could predict the aligned reads abundance associated to each of them using -bamCoverage option. Bigwig files similarity was measured using Deeptools -bigwigcorrelate option. A Pearson correlation was calculated for each compared condition (e.g Sf9 ChIP-seq replicate n°1 against Sf9 ChIP-seq replicate n°2, Sf9 input replicates n°1 against Sf9 ChIP-seq replicate n°1 etc., see Supplementary Fig. S3).

Samtools software allows the reading of SAM files and their concatenation [42]. We merged replicates corresponding the Sf9 ChIP-seq experimental condition to obtain one file for all reads sequenced. Same procedure was applied to Sf9 inputs replicates, L4 ChIP-seq replicates and L4 input.

H3K9me2 whole genome peak detection has been assessed with MACS2 callpeak using the following parameters: --broadpeak -f BAM -g 340000000 -n --down-sample (Y. [97]). Here, MACS2 algorithm predicts large histone peaks detection using a statistical Poisson distribution. Peaks were annotated using Bedtools software (--intersect) after functional annotation of genomic elements. More specifically, the correspondence of H3K9me2 peaks (listed in a Bed files) with the annotation of functional elements (also listed in a Bedfile) was achieved using

Bedtools --intersect option. It allows the recognition of overlapping areas to create a new bedfile. Nucleotide peak comparison between the two models have been performed using online D-genies software [7].

H3K9me2 plot and heatmap over genomic location of interests were produced from Deeptools (computeMatrix and plotHeatmap option).

Integrative Genomic Viewer (IGV) was used for annotation and sequencing track visualization [87].

2.6. Genome functional element annotation

We used published *S. frugiperda* transcriptome [41] for Sf9 and L4 gene annotations using Scipio software [33]. It predicts gene exons by detecting intron/exon junctions with the BLAT algorithm. CDS were reconstructed using Bedtools --groupby function. Introns were annotated by subtracting CDS-exons positions (Bedtools --subtract).

RNA-Seq data were filtered, concatenated et aligned on the genome with the same methods as described for H3K9me2 ChIP-Seq samples. Expression analysis has been performed with Stringtie software ([63]; parameter: stringtie 'bam files' -G genereference.gtf -e). Output in transcript per millions (TPM) was converted to log2 to determine active pool genes (log2(TPM) > 1) from inactive ones (log2(TPM) ≤ 1). Annotation of UTRs in each genome assembly was inconsistent between the different software used (such as Maker, exUTR, getUTR or KLEAT). For the purpose of our metagenome analyses, and based on expression data, we approximated 3'UTRs to be 500bp long after the last exon (bedtools flank -l 0 -r 500 -s), 5'UTRs to be 200 bp long preceding first exon (bedtools flank -l 200 -r 0 -s) and promoters to be 1000 bp long preceding 5'UTRs.

Satellite DNA has been detected using TandemRepeatFinder [3], Repeatexplorer [60] and Repeatmasker on both genomes. Major 150 bp satellite regions were shuffled using Bedtools --shuffle option.

We characterized repeat DNA with consensus sequence inferior or equal to 10 base pairs as microsatellites. Those comprising [10–100]bp where qualified as minisatellites. Finally, consensus sequence satellite of over 100 bp were annotated as satDNA.

We used blastn with default parameters to annotate transposable elements in Sf9 and L4 genomes, using previously determined transposable elements consensus sequences from *S. frugiperda* [22] annotated by the REPET pipeline ([98], sequences with less than 70% homology were filtered out), rDNA copies (with a minimum of 1000 nucleotides length [22]) and telomeres [21] in *Spodoptera* genus.

2.7. Statistic and graphic productions

Barplot, scatterplot, histogram and Venn Diagram were plotted using R software. Student t-test and Chi-square test were performed using R software. Gene ontology enrichment has been performed using BLAST2GO annotations followed by Fisher exact test analysis [9].

3. Results

3.1. H3K9me2 genome-wide distribution in Sf9 and L4 genomes

To investigate the presumptive genome-wide localization of

Table 1
Input and H3K9me2 ChIP-seq sequencing statistics in Sf9 cells and L4 larvae.

Cellular model	Experimental condition	Raw reads	Filtered reads	Unmapped reads	Reads that mapped 1×	Reads that mapped > 1×	Alignment rates
Sf9 cells	Input (1st replicate)	75,090,638	42,741,167	9.36%	46.68%	43.96%	90.64%
	Input (2nd replicate)	75,316,171	19,139,206	8.91%	48.55%	42.54%	91.09%
	H3K9me2 IP (1st replicate)	83,482,976	62,540,058	3.47%	39.22%	57.31%	96.53%
	H3K9me2 IP (2 nt replicate)	35,949,262	23,372,459	3.67%	41.48%	54.85%	96.33%
L4 larvae	Input (1st replicate)	44,093,818	41,023,357	12.42%	70.15%	17.43%	87.58%
	H3K9me2 (1st replicate)	35,076,920	30,539,878	13.56%	60.03%	26.40%	86.44%
	H3K9me2 (2nd replicate)	38,039,481	31,333,074	12.35%	60.61%	27.04%	87.65%

Raw, filtered reads and their alignments using Bowtie 2 Software.

heterochromatin and its dynamic in *S.frugiperda*, we performed ChIP-Seq experiments against the H3K9me2 chromatin mark in Sf9 cells as well as in L4 caterpillars. We first tested the specificity of the mouse anti-H3K9me2 antibody (ab:1220) by immunofluorescence experiments in Sf9 cells. We observed a strong nuclear signal that disappears during metaphase (Supplementary Fig. 1). This is a well-known characteristic of this mark, which is usually shielded by Histone H3 Serine 10 Phosphorylation during mitosis [15,30,64]. We also performed western-blot on chromatin samples showing a 17 kDa band corresponding to the mark in both samples (Supplementary Fig. 2). We then performed ChIP-Seq experiments following an adapted cross-linking procedure for our insect model (see Methods). For each experimental condition (input vs. ChIP-Seq, Sf9 vs. L4) we sequenced two biological replicates, except for L4 input.

After removing short and bad quality sequences, reads were mapped against respective reference genomes for Sf9 cell lines [57] and L4 *S. frugiperda* larvae [55] (Table 1). The alignment rates range between 86.44% and 96.53%. Interestingly, both Sf9 and L4 ChIP-Seq shows a higher level of multimappers (reads mapping more than once) compared to input (Table 1). Indeed, a strong association between H3K9me2 and repeated sequences has been found previously described in Lepidoptera [6,80]. Multimappers number is higher in Sf9 than in L4, probably reflecting differences in genomic assemblies between the two references. Indeed, the Sf9 genome assembly is reported to be 451 Mbp compared to 396 Mbp measured in flow cytometry and 380 Mbp for the L4 genome assembly [55,57]. This excess of sequence in Sf9 assembly may be explained by the polyploidy of these cells [29] leading to unresolved allelic variations in Sf9 and thus in more repeated regions as detected by the higher number of multimappers.

When we tested the similarity of reads enrichment per genomic positions between samples (Supplementary Fig. 3 and detailed in Methods) we observed that Pearson correlation R coefficient is higher between ChIP samples ($R = 0.65$ for Sf9; $R = 0.85$ for larvae) than between Input samples ($R = 0.44$ in larvae), a result consistent with independently sonicated samples.

Since ChIP-Seq and input data segregate separately in both samples (Supplementary Fig. 3), we merged ChIP-seq and Input replicates together and, in both Sf9 and L4 cell models, we analyzed H3K9me2 enrichment by comparing ChIP-Seq over input conditions. Respectively 35,596 and 30,382 peaks of enrichment were found in Sf9 and L4 samples. Half of them were small peaks comprising 0 to ~1000 bp, whereas the other half formed larger genomic domains (comprising between ~1000 bp to several 10,000 bp, Fig. 1A-B). Interestingly, H3K9me2 covers $13.8 \pm 0.02\%$ and $12.6 \pm 0.03\%$ of total Sf9 and L4 genome size. Since our results show relatively equivalent peaks in terms of abundance, distribution length and genomic proportion, we compared raw DNA sequence peak composition (described in Methods) between Sf9 and L4 samples. This analysis retrieved only 11% of homologous peaks in the best case (Supplementary Fig. 4). In order to analyze genome-wide distribution of H3K9me2 enriched domains between samples, we proceeded to the systematic annotation of genes in both *S.frugiperda* and Sf9 genomes, but also the annotation of repeated DNA, including telomeres, rDNA loci as well as transposable elements and satellite DNA (see Methods, Supplementary Table 1). We produced RNA-Seq replicates for Sf9 (see Methods) and reanalyzed published RNA-Seq data of L4 [62] to distinguish a pool of inactive genes from active ones by $\log_2(\text{TPM})$ expression (Supplementary Fig. 5 and Supplementary Table 2).

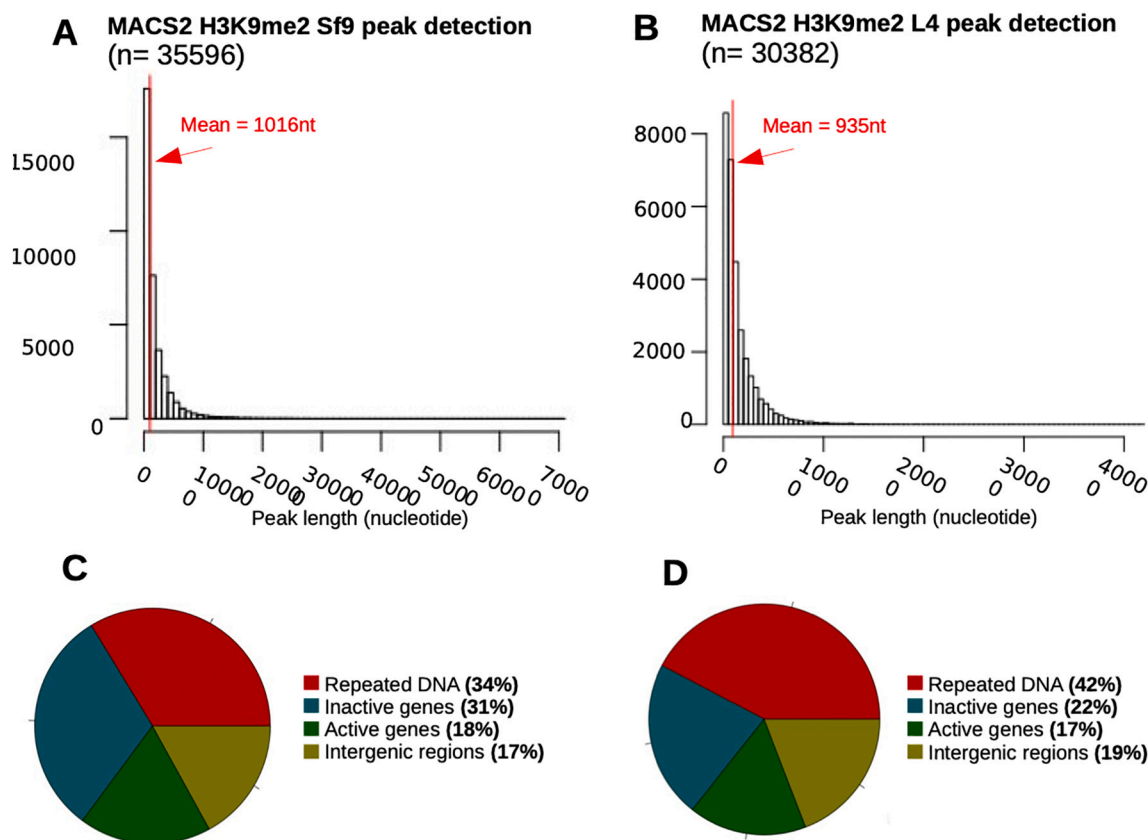


Fig. 1. H3K9me2 genome-wide distribution in *S.frugiperda*.

A-B: Histograms representing H3K9me2 peaks lengths detected by MACS2 in Sf9 reference (A) and L4 reference (B).

C-D: Pie-chart showing compared abundance (%) of annotated H3K9me2 peaks (for repeated DNA, genes and intergenic regions) in Sf9 genome (C) and in L4 genome (D).

Our results show a comparable profile of H3K9me2 functional annotation over both genomes (Fig. 1C-D). The majority of the peaks were found associated with repeated sequences (overall of 34% and 42% in Sf9 and L4) followed by inactive genes (found respectively at 31% and 22% of H3K9me2 peaks). Surprisingly, 18% and 17% of H3K9me2 peaks were also detected within expressed genes. In addition, 17% and 19% peaks were present in intergenic regions.

While our global analysis gives clues about the general distribution of H3K9me2 in *S.frugiperda*, it failed to detect its expected association with telomeres or rDNA locus, with no enrichment found compared to broader regions such as repeated sequences and genes (Supplementary Fig. 6). As this result could be due to a very small fraction of telomeric and rDNA loci in the genome (~80 kb over 400 MB; Supplementary Tables 3 & 4), we specifically analyzed the H3K9me2 distribution around the telomeric regions and rDNA locus (see Results section below) that we annotated in both reference sequences.

3.2. H3K9me2 signal in telomeres repetitions

In Noctuidae, the Lepidoptera family to which belongs the *S.frugiperda* species, chromosome pairs number is stably equal to 31 [69]. Hence, consensual [TTAGG]_n motif constituting telomeres is expected to be annotated at least 62 times in haploid genome assemblies (two tips per chromosome) [21,90]. We searched this motif within the Sf9 and L4 genomes, and respectively detected it in 108 and 63 regions (Supplementary Table 3). For each presumptive telomeric region, we checked whether it was associated with any H3K9me2 peak. Fig. 2A shows an example of homologous telomeres found in distinct Sf9 and L4 references. Homology was verified by the presence of the same upstream gene. Global analysis of these regions showed that 62 and 57 copies were enriched in H3K9me2 over the 108 and 63 annotated, representing $57 \pm 9.3\%$ and $90 \pm 7.4\%$ of Sf9 and L4 H3K9me2 telomere coverage (Fig. 2B). In other biological models, ncRNA corresponding to telomeres have been found [73]. However, regardless of their length, [TTAGG]_n motif sequences have almost no mapped transcripts in our samples (Fig. 2C).

3.3. H3K9me2 signal in rDNA locus

Previous FISH cytology experiments conducted in Noctuidae showed the conservation of one rDNA locus located interstitially in an autosome [59]. This polycistronic-like cluster is made of repeated 18S, 5.8S and 28S genes with additional 5S RNA being anti-sense included or extra located [76]. In case of low translational activity, some rDNA copies are heterochromatinized with H3K9me2 mark [79]. Like we did for telomere sequences, we compared H3K9me2 enrichment and transcription at rDNA loci. We searched both reference genomes for rDNA sequences and found one major locus in both, even though relatively shorter rDNA sequences and even larger ones can be detected at various places in the genome (Supplementary Table 4). The homologous rDNA regions in Sf9 and L4 genomes are highly transcribed with respective mean coverage values of 78.51 X and 320.7 X, even though RNA-Seq has been performed by mRNA enrichment through ribosomal DNA depletion (Fig. 3A). Intriguingly, we observed in Sf9 a co-occurrence of H3K9me2 enrichment and high RNA transcription (Fig. 3A, upper panel). This counterintuitive result can be explained by sequence nature: since rDNA clusters are made of the same repeated sequences, short reads can align to heterochromatinized domains as well as euchromatic ones. Thus, if only one or few portions are H3K9me2 enriched in biological reality, every identical DNA sequence would be predicted as associated with the mark. The results are more coherent in L4 with RNA expression coinciding with absence of H3K9me2 peak. rDNA expression is even found overexpressed when comparing the rDNA cluster to a pool of active genes (Fig. 3B, Student *t*-test, *p*value <2.2x10⁻¹⁶).

3.4. H3K9me2 enrichment around satellite DNA regions

In many organisms, heterochromatin is associated with pericentromeric regions ([28,83], Supplementary Fig. 7). These regions can be quite large, spanning several Mb of sequences [68]. We wondered whether heterochromatin in holocentric species is also associated with pericentric regions. To detect putative centromeres in *S.frugiperda*, we searched and annotated satellite DNA sequences [82]. Indeed, a previous molecular evolution study conducted on 282 species showed that the most abundant 150 bp satellite repetitions present in the genome correspond to centromeric DNA sequences [50]. This was confirmed for the majority of monocentric organisms but contested for holocentric ones [50] with only *Rynchospora pubera* plant sharing this characteristic [49]. We searched the most abundant 150 bp satDNA in *S.frugiperda* and analyzed its chromosomal distribution, its transcriptional status and its peripheral H3K9me2 enrichment.

Our analysis (see Methods) identified one 150 bp satellite DNA (satDNA) consensus sequence shared between Sf9 and L4 (Fig. 4A). This repeated sequence is found in 1184 and 1238 copies within Sf9 and L4 genomes respectively (Fig. 4B). These satDNA regions do not overlap any previously annotated functional sequences (telomere, rDNA, genes etc.). Their median length is between 281 and 292 base pairs, which could correspond to 2 nucleosomes. Transcription rates were found lower or similar to annotated telomeres or the pool of inactive genes in both references (Fig. 4C, Student *t*-test). Interestingly, H3K9me2 enrichment profile around satDNA was found similar in the two references with a systematic decrease of the mark inside candidate sequences opposing a broader adjacent signal. When candidate sequences are shuffled for genomic localization, no H3K9me2 enrichment is detected in and around regions of interest (Supplementary Fig. 8), confirming that H3K9me2 association with satDNA is not random. In both references, highest adjacent H3K9me2 peaks are stably found around 1000 bp from major 150 bp satellites (Fig. 4D). While this result might indicate an association of heterochromatin with centromeric regions in holocentric species, additional studies would be needed to confirm that satDNA corresponds to bona fide centromeres in *S. frugiperda*.

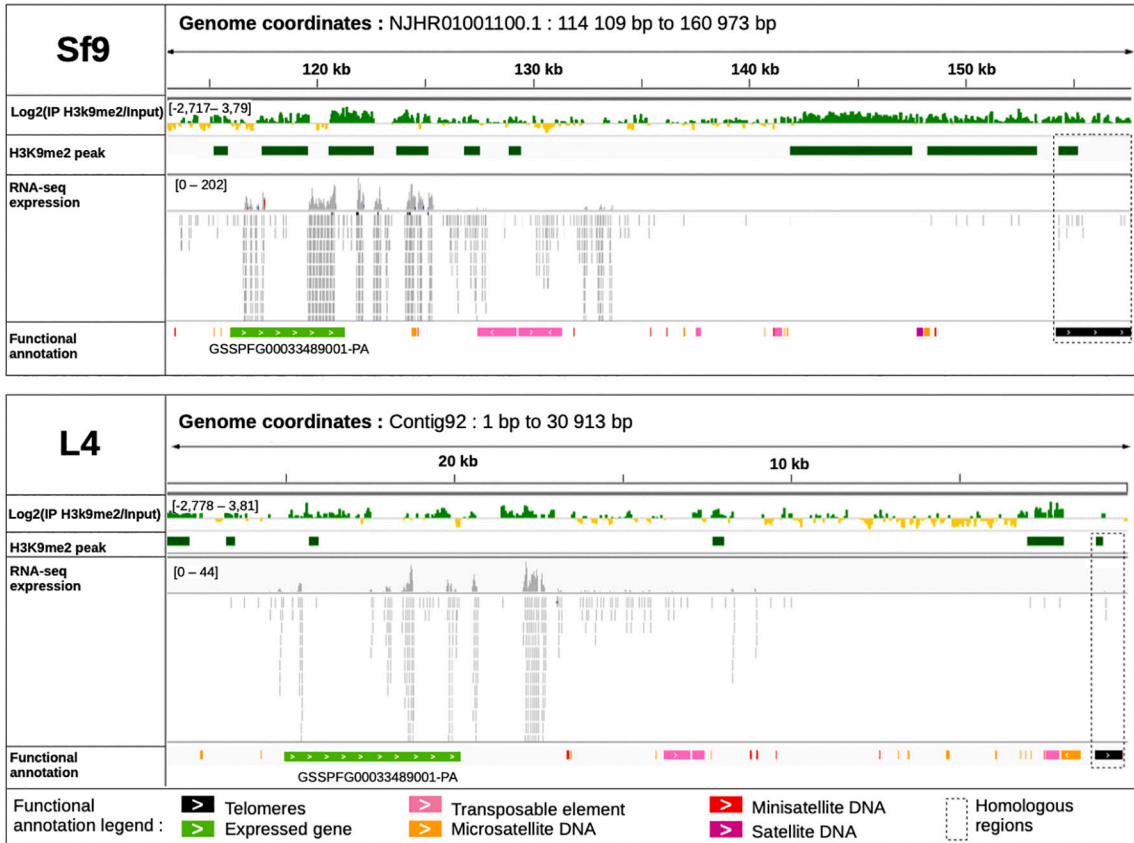
3.5. H3K9me2 enrichment in repeat elements families

Between 34% to 42% of H3K9me2 peaks are associated with repeat sequences (Fig. 1C,D). We annotated in both reference genomes the different categories of repeat sequences, whether they correspond to tandem repeats, such as micro- and mini- satellite sequences, or transposable elements (Fig. 5A). We found around a hundred thousand micro- and minisatellite sequences in both Sf9 and L4 genome assemblies, representing 3,674,661 / 2,875,505 bp and 1,706,018 / 1,149,269 bp each, or about 0.7% and 0.3% of the genome. We found less satellite sequence repeats (1719 and 3067 sequences) representing 0.5% and 0.2% of the genome but a large amount of putative transposable elements (46,625 and 55,928 sequences representing 6.7% and 9.8% of the genome).

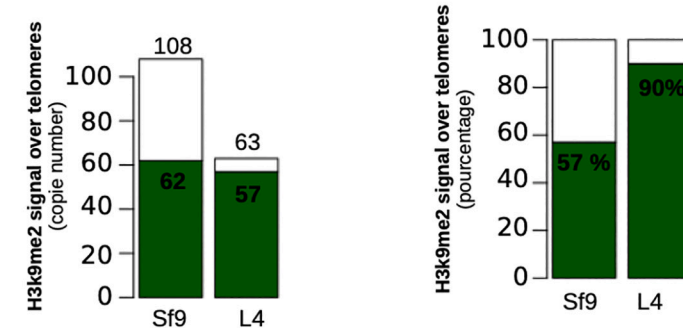
We then calculated the proportion of each category associated with H3K9me2 (Fig. 5A). A higher proportion of satellite sequences and transposable elements is found associated with H3K9me2 compared to micro- and mini-satellite, which agrees with our expectation of a role of heterochromatin associated with repeat-rich regions of the genome.

The higher prevalence of repeat DNA and transposable elements in c-Het compartments in model organisms is often explained by the repressive nature of heterochromatin. Indeed, because of their potential deleterious effects on the genome when they are mobilized, transposable elements are often transcriptionally repressed by small RNA targeted H3K9me ([35,77]; Le [39]). In order to determine if a similar role of H3K9me2 exists in *S. frugiperda*, we analyzed the RNA-Seq data from L4 tissues and Sf9 cells to classify transcribed and non-transcribed transposable elements and observe the association of each category with H3K9me2 signal (Fig. 5B). No enrichment was observed, with H3K9me2

A



B



C

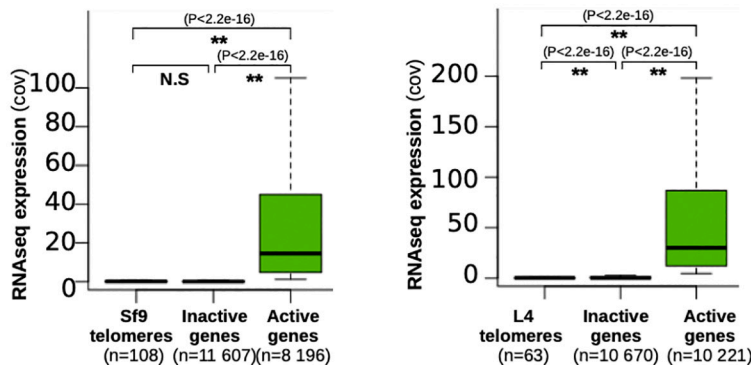


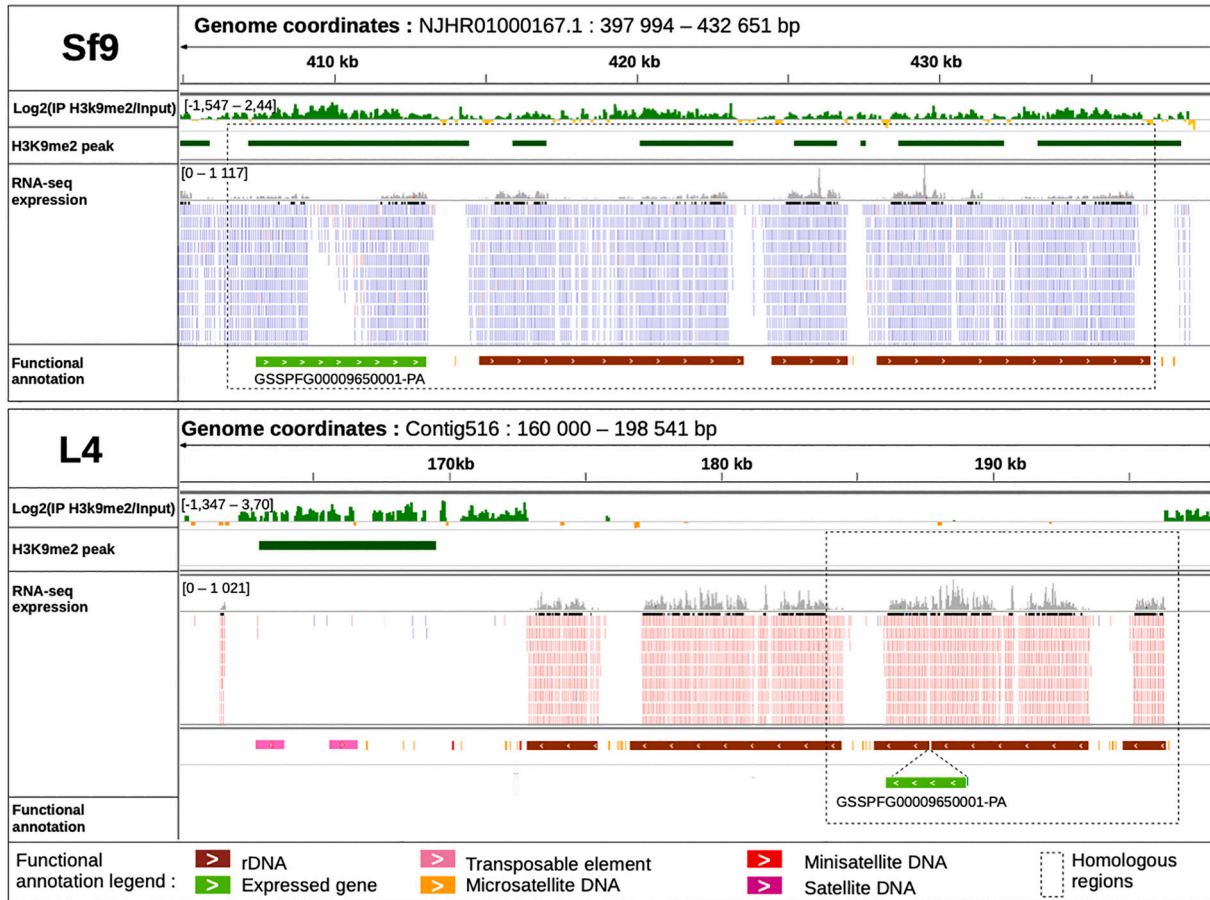
Fig. 2. Analysis of H3K9me2 in telomeres.

A: IGV view of homologous telomere copies found in Sf9 cells (top) and L4 (bottom). From the top to bottom of each view, the following tracks are displayed: 1) log2 (input/H3K9me2) bigwig file (bins = 50 bp), 2) H3K9me2 peaks, 3) RNA-Seq track, 4) Annotated functional element (genes, repeated DNA).

B: H3K9me2 peak abundance in telomere annotated copies (top). Same result is shown with percentages (bottom).

C: RNA-Seq expression boxplot comparison between putative telomeres, inactive genes and active genes are shown for Sf9 (left) and L4 (right). Statistical significance has been assessed by t-test. (*): $P < 0,05$; (**): $P < 0,001$, NS: non-significant.

A



B

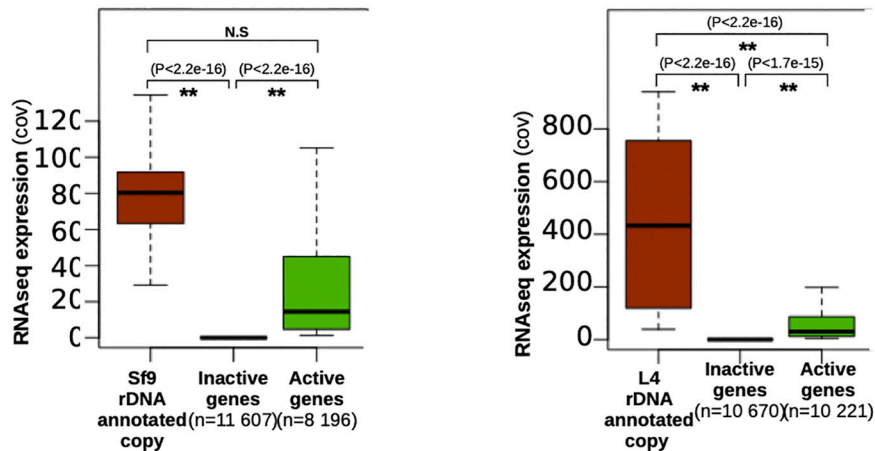


Fig. 3. Analysis of H3K9me2 in repeated ribosomal locus.

A: IGV view of the rDNA copies found in Sf9 cells (top) and L4 (bottom). Tracks from top to bottom are: 1) log2(input/H3K9me2) bigwig file (bins = 50 bp), 2) H3K9me2 peaks, 3) RNA-Seq track, 4) Annotated functional element (genes, repeated DNA).

B: RNA-Seq expression boxplot comparison between rDNA, inactive genes and active genes are shown for Sf9 (left) and L4 (right). Statistical significance has been assessed by t-test. (*): $P < 0,05$; (**): $P < 0,001$, NS: non-significant.

being equally found between active and inactive transposable elements.

3.6. H3K9me2 signal enrichment in genes

Due to the classical repressive nature of heterochromatin, we expected H3K9me2 to be associated with mainly inactive genes. This was indeed the case in both references even if we observed unexpected

H3K9me2 enrichments into pools of active genes (Fig. 1B).

We analyzed if some gene regions like promoters, UTRs or gene bodies were more enriched in H3K9me2 than others (Fig. 6A). We found inactive promoters to be statistically more associated with H3K9me2 than active promoters in the two references (Sf9: $\chi^2 = 317.37$, $df = 1$, p -value<2.2e-16; L4: $\chi^2 = 667.97$, $df = 1$, p -value<2.2e-16). However, 16% Sf9 and 26% L4 active promoters were also associated with

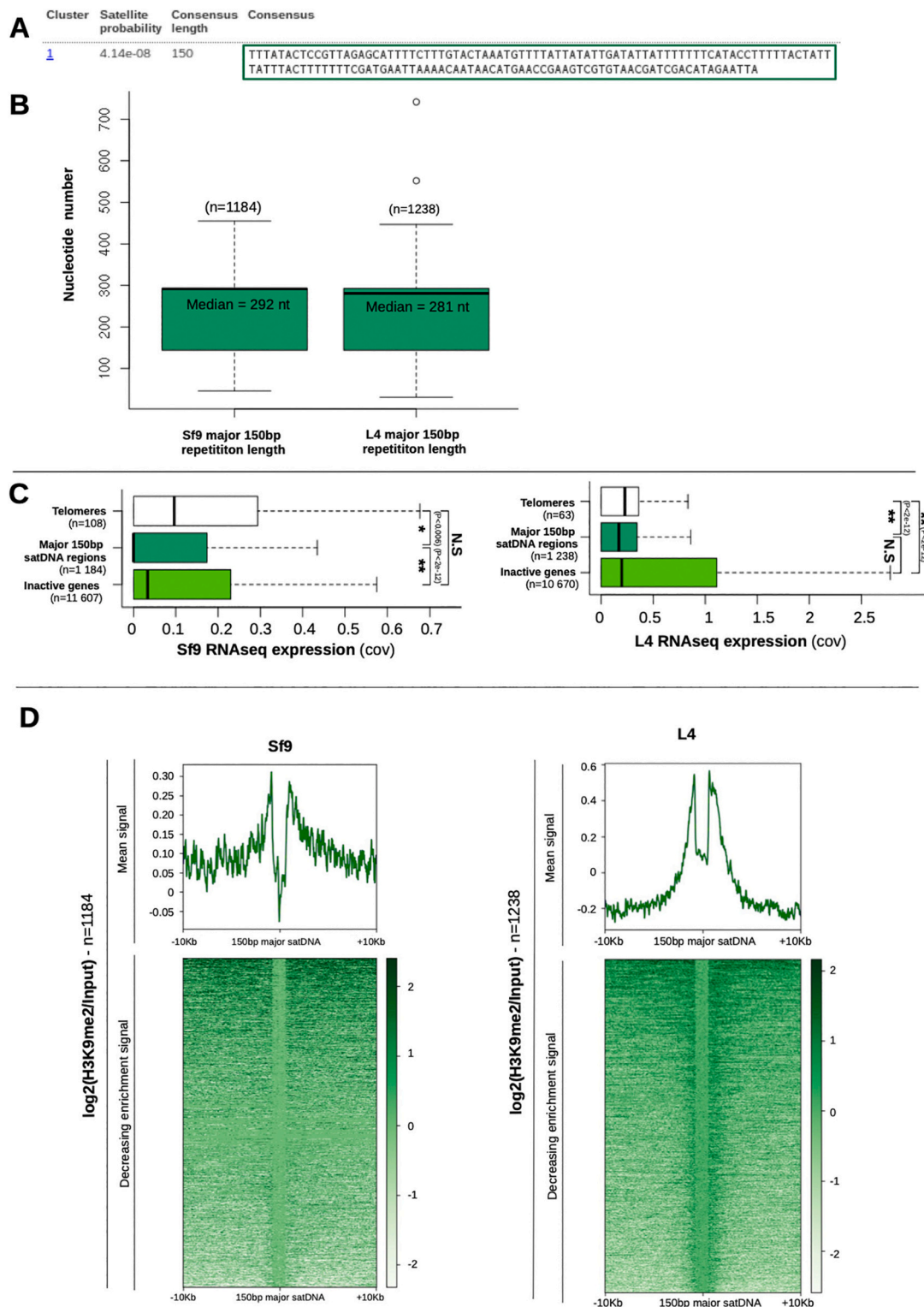


Fig. 4. Analysis of H3K9me2 around most abundant 150 bp satDNA repeat.

A: Table showing first rank 150 bp satDNA detected in Sf9 and L4 genome by RepeatExplorer. Probability, consensus length and DNA sequence composition are indicated.

B: Boxplot of 150 bp satDNA repetition regions length in Sf9 (left) and L4 (right).

C: Boxplot of RNA-Seq expression (in cov, x-axis) between telomeres, 150 bp candidate regions and inactive genes of Sf9 (left) and L4 (right). Statistical significance of expression has been assessed by t-test. (*): $P < 0,05$; (**): $P < 0,001$, NS: non-significant.

D: H3K9me2 expression of peripheral major 150 bp satDNA regions in Sf9 (left) and L4 (right).

For upper graphs: Mean $\log_2(\text{H3K9me2}/\text{Input})$ signal (y-axis) in 10 kb regions surrounding region of interest (x-axis).

For lower graphs: Decreasing $\log_2(\text{H3K9me2}/\text{Input})$ expression (y-axis) of 150 bp satDNA regions and 10 kb around (x-axis).

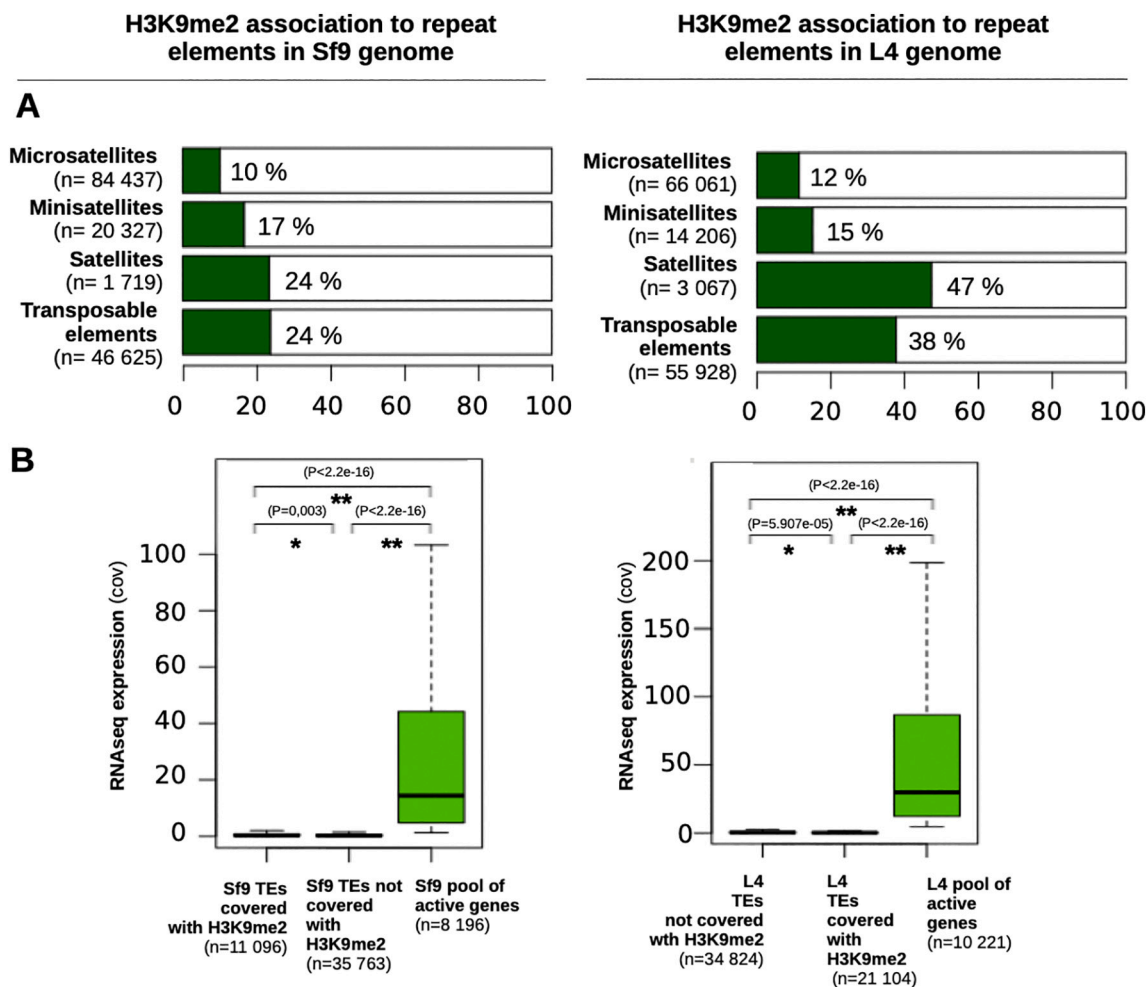


Fig. 5. Analysis of H3K9me2 enrichment with repeat element families.

A: Plots showing abundance (in %, x-axis) of H3K9me2 in annotated tandem repeats and transposable elements of Sf9 (left) and L4 (right) genomes.

B: Boxplot comparing transposable elements RNA-Seq expression between those covered with H3K9me2, others without epigenetic mark association and pool of active genes.

H3K9me2 marks, which may be due to the cell heterogeneity in both samples or to difficulties in promoter prediction in our model. H3K9me2 is also detected within the gene body and UTRs regardless of the gene transcriptional status in equivalent proportions between Sf9 and L4 cells (Fig. 6A). Interestingly, when we took a further look into differently H3K9me2 enriched for gene body regions, we observed a more intense signal in exons compared to introns.

In Sf9 cells, 42.8% of annotated genes are associated with H3K9me2 and 39.1% in L4 (Fig. 6B). For those genes, H3K9me2 signal is distributed within exons rather than introns (Fig. 7). Two-thirds of the H3K9me2 covered genes regardless of their transcription state are shared between the two references (Fig. 6B). For these common genes, we performed a Gene Ontology analysis. We observed an enrichment in functions associated with transposable elements regulation (Supplementary Fig. 9, GO: endonuclease activity, nuclease activity) and nucleic acid homeostasis (Supplementary Fig. 9, GO: DNA metabolic process, catalytic activity acting on DNA etc.). We also noticed the presence of genes involved in heterochromatin maintenance and formation, suggesting possible molecular feedback. It includes a H3K9me methyltransferase enzyme (Suvar3/9: GSSPFG00004579001-PA, G9a: GSSPFG00019340001.2-PA), DNA methylase enzyme (DNMT1 (GSSPFG00025486001.2-PA)), centromere formation proteins (search from [10]; inner kinetochore: CENP-P (GSSPFG00001205001-PA)), ATP synthase subunit (GSSPFG00010096001-PA; [8]), outer kinetochore: Nuf2 (GSSPFG00010779001-PA), BLAST2Go annotated centromeric

proteins (GSSPFG00020169001-PA, GSSPFG00005386001.4-PA)) and HP1 family proteins (HP1c (GSSPFG00011657001.2-PA), HP1e (GSSPFG00007777001.2-PA)). Paradoxically, lots of spliceosome genes involved in active transcription and mRNA formation are also found.

4. Discussion

We report the first H3K9me2 genome-wide ChIP-Seq analysis conducted in *S. frugiperda*, a lepidopteran species. Our results are globally consistent with previous studies on H3K9me2 [26] albeit with a higher percentage of genome covered ($13.8 \pm 0,02\%$ and $12,6 \pm 0,03\%$ in Sf9 and L4) than in other monocentric and holocentric organisms, maybe due to genome assemblies in our model spanning scattered heterochromatic regions usually not assembled in organisms with large pericentromeric regions [68]. In both genome assemblies, we detected H3K9me2 at expected chromosomal compartments such as telomeres and rDNA locus but no major centromeric locus. Instead, we observed a scattered distribution of H3K9me2 along the chromosomes colocalizing with genes and repeat elements, independent of their transcriptional status. Qualitatively H3K9me2 distribution along Sf9 and L4 models shows the same patterns with exact same rank of functional categories represented. Indeed, repetitive DNA comes first as the most enriched category for the mark. Then, inactive genes and active genes plus intergenic regions come last. Quantitatively the differences are harder to address since we aligned the ChIP-seq experiments against

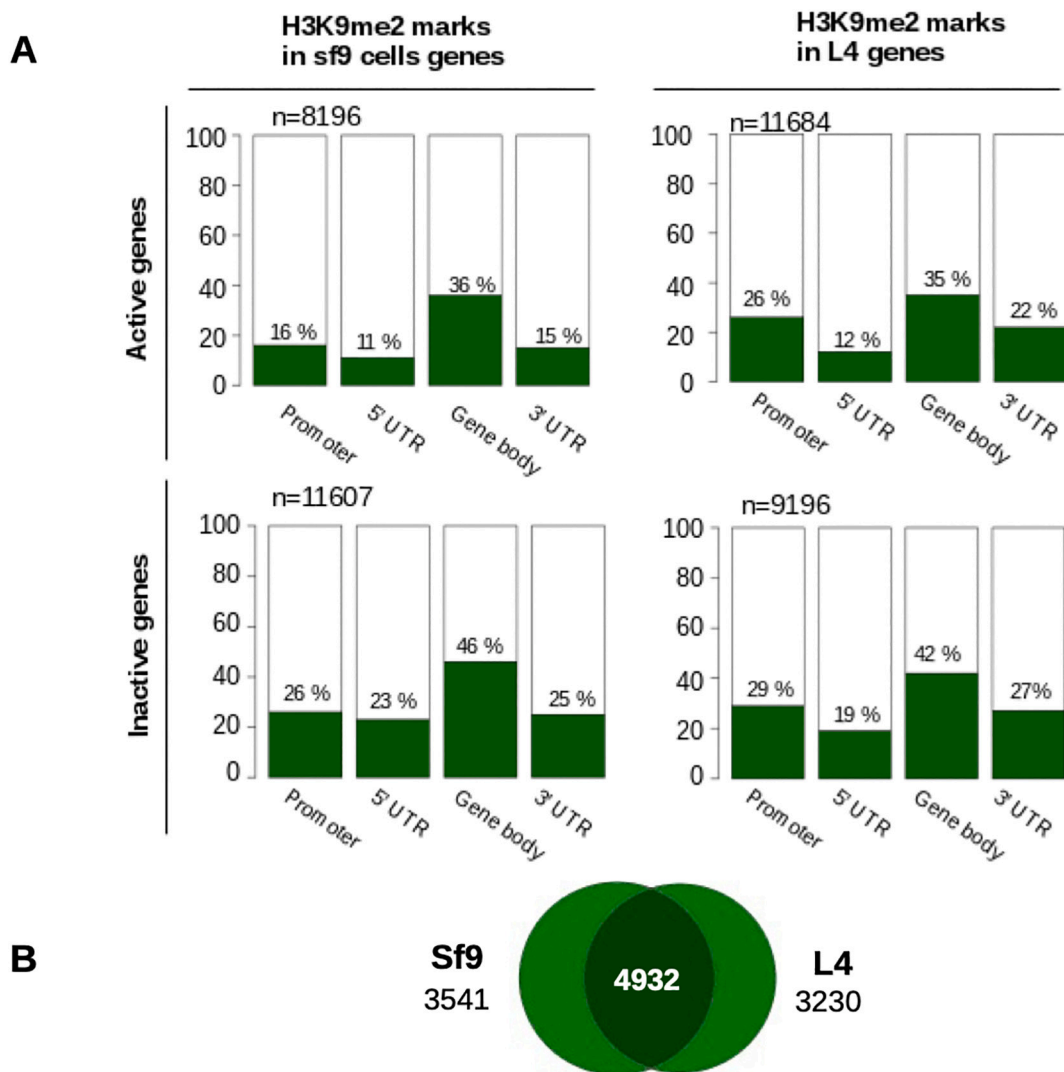


Fig. 6. Analysis of gene regions covered with H3K9me2 mark.

A: Plots showing abundance (in %, y-axis) of H3K9me2 present in promoters, UTRs and CDS (x-axis) of active genes (upper part) vs. inactive genes (lower part) from Sf9 (left) and L4 (left) cell models.

B: Venn diagram showing unique genes respectively covered in Sf9 and L4 (left and right part) and common ones (middle part).

independently assembled genomes (Sf9 genome shows twice more scaffolds than L4 ones), with H3K9me2 peaks found in more abundance in Sf9 compared to L4 (35,596 against 30,382 peaks). The difference of active vs. inactive gene enrichment for H3K9me2 could be explained by a putative difference in gene regulation of the respective cell models (Supplementary Fig. 5).

4.1. Localization of H3K9me2 at expected heterochromatin compartments

In many monocentric organisms, c-Het is found in large regions surrounding the centromere. Since we found H3K9me2 to be still associated with heterochromatin domains such as telomeres or rDNA locus in *S. frugiperda* (Figs. 2,3), we hypothesized that c-Het could also identify putative centromeric regions in this holocentric specie. As mentioned in the introduction, H3K9me2 surrounding the major 150 bp satDNA repetition is a conserved pattern for pericentric regions in monocentric species. To retrieve putative centromeric regions in the genome of *S. frugiperda*, we annotated the most abundant 150 bp satDNA and found it present in more than a thousand scattered copies in both genomes (Fig. 4). Since we also observed an enrichment of H3K9me2 within 1 kb

of satDNA, we hypothesize they could represent holocentromeres. A recent publication on lepidopteran cell lines (*Bombyx mori* and *Trichoplusia ni*) describes centromeres marked by the centromeric protein CenP-T to be unusually associated with the facultative heterochromatin mark H3K27me3 [10,75]. However, the distribution of H3K9me2 was not assessed in their study and we don't know whether it colocalizes with H3K27me3 or is excluded. It is possible that satDNA sequences associated with H3K9me2 represent in fact vestigial centromeres that stopped being used by the cell after H3K27me3 replacement. To determine if such genomic regions correspond to functional holocentromeres, its association with kinetochore proteins would have to be demonstrated.

4.2. Repeated sequences and H3K9me2 association

Among the conserved features of H3K9me2 distribution, we observed this mark to be mainly associated with repeated DNA sequences in both cellular references. This was evidenced by the high abundance of multimapper reads in both cellular references (Table 1) but also by the significant ChIP enrichment on the different categories of annotated repeated DNA (Fig. 1C). While this association was expected

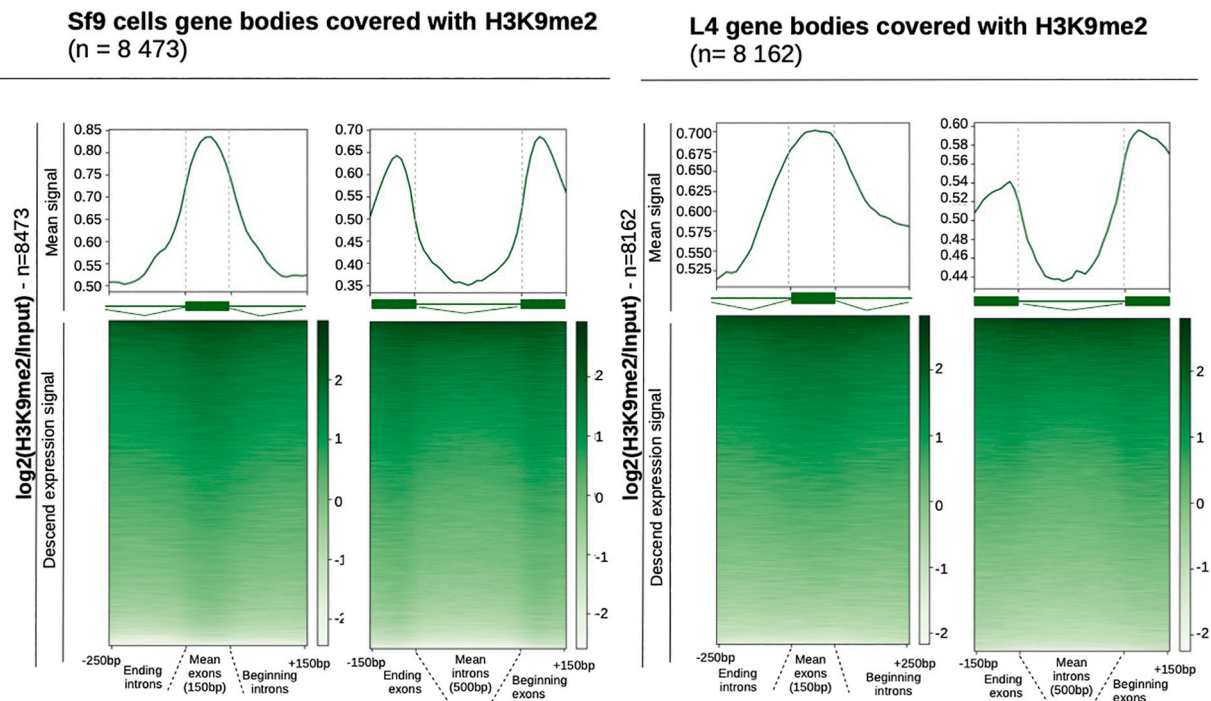


Fig. 7. Analysis of H3K9me2 signal covering exons vs introns gene bodies. Left: Sf9; Right: L4. For upper graphs: Mean $\log_2(\text{H3K9me2}/\text{Input})$ signal (y-axis) in all exons (left) and introns (right, x-axis). For lower graphs: Ascend $\log_2(\text{H3K9me2}/\text{Input})$ expression (y-axis) in all exons (left) and introns (right, x-axis).

from previous studies conducted in Lepidoptera [6,80], we present here a more exhaustive association with the different categories of repeats. However, we did not observe a complete association of the mark with repeat elements with only 24% and 38% of transposable elements intersecting H3K9me2 peaks (Fig. 5A). Furthermore, we did not observe a clear correlation between transposable elements repression and H3K9me2 as we were expecting ([35], Fig. 5B). Without a well-defined pericentric heterochromatin compartment, it is possible that in Lepidoptera piRNA directed chromatin repression of transposable elements is achieved through other mechanisms. Future genome-wide H3K27me3 or H3K9me1/3 ChIP-Seq data should be compared with H3K9me2 to determine if, in Lepidoptera, transposable elements control is insured by similar heterochromatin mechanisms as in other model insects.

4.3. H3K9me2 association with genes bodies

H3K9me2 in *S.frugiperda* is associated with some gene bodies regardless of their active or inactive transcriptional status (Fig. 1B). This histone mark has been described to cover coding sequences in two different situations.

The first situation corresponds to hundreds of genes that are present in c-Het compartments. Contrary to silenced euchromatic genes at heterochromatin proximity -an effect called position effect variegation (PEV, [91])- these heterochromatic genes do not function when displaced in euchromatin [13,70,94]. Their expression is compatible with H3K9me2 covering. Principally described in drosophila, some of these genes are essential for development and are mainly concentrated in pericentromeric regions. Given their localization, they are thought to be more prone to transposable elements insertions and show lots of intronic transposons. In *S.frugiperda*, we identified more than 4900 genes associated with the H3K9me2 mark. Their function reflects constitutive roles such as general transcription factors, ribosomal genes or mitochondrial genes, which fits with heterochromatic genes hypothesis.

The second situation described in the literature of H3K9me2 association with gene bodies is in alternative splicing. Presence of exonic H3K9me2 across genes is thought to slow down polymerase in order to

favor alternative instead of constitutive mRNA transcription [71]. Consistent with this, our analysis of H3K9me2 signal in *S.frugiperda* shows a higher enrichment in exons compared to introns (Fig. 7). In order to confirm a splicing role for this mark in *S.frugiperda*, it would be necessary to annotate exons nature (internal vs. external, constitutive vs. alternative, etc.) and check if alternative mRNA transcripts are produced given presence or absence of exonic H3K9me2 signal. If previous studies focused on other heterochromatic components such as DNA methylation or HP1c proteins to regulate transcription et alternative splicing in insects [5,43], no studies linking these epigenetic factors with H3K9me2 has been addressed in Lepidoptera. This fact is important since HP1c is usually described on both exons and introns. A recent work revealed intronic HP1c signal to be involved in alternative splicing through binding with abundant “CACACA” intronic repeated motif sequences [65]. Our search for a similar motif in *S.frugiperda* using two dedicated softwares failed to give the same results. But a systematic association of HP1c and H3K9me2 cannot be assessed since HP1c can bind to other modified marks and RNAs. In addition, the correspondence of classical HP1 proteins with homologs in Lepidoptera is not clear. In *B. mori*, two HP1 homologs have been described: BmHP1a and BmHP1b [53]. We also retrieved those two homologs in *S.frugiperda* genomes even though the phylogeny needs to be more resolved since they are not on the same branch as the classical *Drosophila* HP1a (Supplementary Fig. 10).

5. Conclusion / Article summary

We produced the first genome-wide analysis of holocentric Lepidoptera *S. frugiperda* heterochromatin distribution by analyzing H3K9me2 ChIP-Seq data in two cell models. In contrast to studies suggesting unusual behavior of modified histones, our results supported a conserved pattern with invariant classic c-Het domains such as (sub) telomeres, rDNA locus and even peripheral major 150 bp satDNA that could be associated with centromeric functions. However, since H3K9me2 is abundantly present in transposable elements as well as gene bodies regardless of their expression status, it could either reflect a pleiotropic function of H3K9me2 or a vestigial distribution due to the

loss of a pericentromeric compartment. In order to deepen these results and get a more detailed picture of heterochromatin localization in holocentric Lepidoptera, further work characterizing other associated histone marks, DNA methylation and HP1 proteins genome-wide distribution in Lepidoptera will be required.

Authors contributions

SN, EA and NN designed the project and the experiments, SG, SN and RNS performed the Western-Blot, Immuno-fluorescence and ChIP experiments, DS produced the Illumina libraries and sequencing. SN produced the bioinformatic and statistical analysis with the help of KWN. SN and NN wrote the manuscript with the input of all co-authors.

Acknowledgements

This work was supported by a grant from the French National Research Agency (ANR-12-BSV7-0004-01; <http://www.agence-nationale-recherche.fr/>) for EA and Institut Universitaire de France for NN. The funding bodies had no role in the design of the study and collection, analysis, and interpretation of data and in writing the manuscript.

Appendix A. Supplementary data

Supplementary data to this article can be found online at <https://doi.org/10.1016/j.ygeno.2021.12.014>.

References

- Emmanuelle d'Alençon, Nicolas Nègre, Slavica Stanojic, Benjamin Allassoer, Sylvie Gimenez, Alexandre Léger, Adly Abd-Alla, Sylvie Juliant, Philippe Fournier, Characterization of a CENP-B homolog in the holocentric lepidoptera *Spodoptera frugiperda*, *Gene* 485 (2) (2011) 91–101, <https://doi.org/10.1016/j.gene.2011.06.007>.
- Robin C. Allshire, Hiten D. Madhani, Ten principles of heterochromatin formation and function, *Nat. Rev. Mol. Cell Biol.* 19 (4) (2018) 229–244, <https://doi.org/10.1038/nrm.2017.119>.
- G. Benson, Tandem repeats finder: A program to analyze DNA sequences, *Nucleic Acids Res.* 27 (2) (1999) 573–580, <https://doi.org/10.1093/nar/27.2.573>.
- Holger Bierhoff, Anna Postepska-Igielska, Ingrid Grummt, Noisy silence: non-coding RNA and heterochromatin formation at repetitive elements, *Epigenetics* 9 (1) (2014) 53–61, <https://doi.org/10.4161/epi.26485>.
- Roberto Bonasio, Qiye Li, Jinmin Lian, Navdeep S. Mutti, Lijun Jin, Hongmei Zhao, Pei Zhang, et al., Genome-wide and caste-specific DNA methylomes of the ants *Camponotus floridanus* and *Harpegnathos saltator*, *Curr. Biol.* 22 (19) (2012) 1755–1764, <https://doi.org/10.1016/j.cub.2012.07.042>.
- Federica Borsatti, Mauro Mandrioli, Conservation of HP1 and Methylated H3 histones as heterochromatic epigenetic markers in the holocentric chromosomes of the Cabbage Moth, *Mamestra brassicae* (Lepidoptera), *Eur. J. Entomol.* 102 (4) (2005) 625–632, <https://doi.org/10.14411/eje.2005.088>.
- Floréal Cabanettes, Christophe Klopp, D-GENIES: dot plot large genomes in an interactive, efficient and simple way, *PeerJ* 6 (juin) (2018), <https://doi.org/10.7717/peerj.4958> e4958.
- Caitriona M. Collins, Beatrice Malacrida, Colin Burke, Patrick A. Kiely, Elaine M. Dundleavy, ATP synthase F1 subunits recruited to centromeres by CENP-A are required for male meiosis, *Nat. Commun.* 9 (1) (2018) 2702, <https://doi.org/10.1038/s41467-018-05093-9>.
- Ana Conesa, Stefan Götz, Juan Miguel García-Gómez, Javier Terol, Manuel Talón, Montserrat Robles, Blast2GO: a universal tool for annotation, visualization and analysis in functional genomics research, *Bioinformatics* 21 (18) (2005) 3674–3676, <https://doi.org/10.1093/bioinformatics/bti610>.
- Nuria Cortes-Silva, Jonathan Ulmer, Takashi Kiuchi, Emily Hsieh, Gaetan Cornilleau, Ilham Ladid, Florent Dingli, Damarys Loew, Susumu Katsuma, Ines A. Drinnenberg, CenH3-independent kinetochore assembly in lepidoptera requires CCAN, including CENP-T, *Curr. Biol.* 30 (4) (2020) 561–572, e10, <https://doi.org/10.1016/j.cub.2019.12.014>.
- Bernard Crespi, Patrik Nosil, Conflictual speciation: species formation via genomic conflict, *Trends Ecol. Evol.* 28 (1) (2013) 48–57, <https://doi.org/10.1016/j.tree.2012.08.015>.
- Niall Dillon, Heterochromatin structure and function, *Biol. Cell.* 8 (8) (2004) 631–637, <https://doi.org/10.1016/j.biolcel.2004.06.003>.
- Patrizio Dimitri, Ruggiero Caizzi, Ennio Giordano, Maria Carmela Accardo, Giovanna Lattanzi, Giuseppe Biamonti, Constitutive heterochromatin: a surprising variety of expressed sequences, *Chromosoma* 118 (4) (2009) 419–435, <https://doi.org/10.1007/s00412-009-0211-y>.
- Ines A. Drinnenberg, Dakota de Young, Steven Henikoff, Harmit Singh Malik, Recurrent loss of CenH3 is associated with independent transitions to holocentricity in insects, *Ed. Anthony A Hyman, eLife* 3 (septembre) (2014), <https://doi.org/10.7554/eLife.03676>. e03676.
- Qing Duan, Haobin Chen, Max Costa, Wei Dai, Phosphorylation of H3S10 blocks the access of H3K9 by specific antibodies and histone methyltransferase, *J. Biol. Chem.* 283 (48) (2008) 33585–33590, <https://doi.org/10.1074/jbc.M803312200>.
- Marcial Escudero, J. Ignacio Márquez-Corro, Andrew L. Hipp, The phylogenetic origins and evolutionary history of holocentric chromosomes, *Syst. Bot.* 41 (3) (2016) 580–585, <https://doi.org/10.1600/036364416X692442>.
- Patrick M. Ferree, Daniel A. Barbash, Species-specific heterochromatin prevents mitotic chromosome segregation to cause hybrid lethality in *Drosophila*, *PLoS Biol.* 7 (10) (2009), <https://doi.org/10.1371/journal.pbio.1000234> e1000234.
- Reto Gassmann, Andreas Rechtsteiner, Karen W. Yuen, Andrew Muroyama, Thea Egelhofer, Laura Gaydos, Francie Barron, et al., An inverse relationship to germline transcription defines centromeric chromatin in *C. elegans*, *Nature* 484 (7395) (2012) 534–537, <https://doi.org/10.1038/nature10973>.
- Jean-Michel Gibert, Emmanuèle Mouchel-Vielh, Sandra De Castro, Frédérique Peronnet, Phenotypic plasticity through transcriptional regulation of the evolutionary hotspot gene *tan* in *Drosophila melanogaster*, *PLoS Genet.* 12 (8) (2016), <https://doi.org/10.1371/journal.pgen.1006218> e1006218.
- Georg Goergen, P. Lava Kumar, Sagnia B. Sankung, Abou Togola, Manuele Tamò, First report of outbreaks of the fall armyworm *Spodoptera frugiperda* (J E Smith) (Lepidoptera, Noctuidae), a New Alien Invasive pest in West and Central Africa, *PLoS One* 11 (10) (2016), <https://doi.org/10.1371/journal.pone.0165632>.
- H. Gong, W. Zhu, J. Zhang, X. Li, Q. Meng, G. Zhou, M. Wang, et al., TTAGG-repeat telomeres and characterization of telomerase in the beet armyworm, *Spodoptera exigua* (Lepidoptera: Noctuidae), *Insect Mol. Biol.* 24 (3) (2015) 358–367, <https://doi.org/10.1111/imb.12163>.
- Anais Gouin, Anthony Bretaudeau, Kiwoong Nam, Sylvie Gimenez, Jean-Marc Aury, Bernard Duvic, Frédérique Hilliou, et al., Two genomes of highly polyphagous lepidopteran pests (*Spodoptera frugiperda*, Noctuidae) with different host-plant ranges, *Sci. Rep.* 7 (1) (2017), <https://doi.org/10.1038/s41598-017-10461-4>.
- Shiv I.S. Grewal, Songtao Jia, Heterochromatin revisited, *Nat. Rev. Genet.* 8 (1) (2007) 35–46, <https://doi.org/10.1038/nrg2008>.
- Heitz E. Das, Heterochromatin der Moose, *Jahrb Wiss Botanik* 69, 1928, pp. 762–818.
- Steven Henikoff, Kami Ahmad, Harmit S. Malik, The centromere paradox: stable inheritance with rapidly evolving DNA, *Science* 293 (5532) (2001) 1098–1102, <https://doi.org/10.1126/science.1062939>.
- Joshua W.K. Ho, Youngsook L. Jung, Tao Liu, Burak H. Alver, Soohyun Lee, Kohta Ikegami, Kyung-Ah Sohn, et al., Comparative analysis of metazoan chromatin organization, *Nature* 512 (7515) (2014) 449–452, <https://doi.org/10.1038/nature13415>.
- Stacie E. Hughes, R. Scott Hawley, Heterochromatin: A rapidly evolving species barrier, *PLoS Biol.* 7 (10) (2009), <https://doi.org/10.1371/journal.pbio.1000233>.
- Aniek Janssen, Serafin U. Colmenares, Gary H. Karpen, Heterochromatin: guardian of the genome, *Annu. Rev. Cell Dev. Biol.* 34 (octobre) (2018) 265–288, <https://doi.org/10.1146/annurev-cellbio-100617-062653>.
- R.F. Jarman-Smith, S.J. Armstrong, C.J. Mannix, M. Al-Rubeai, Chromosome instability in *spodoptera frugiperda* Sf-9 cell line, *Biotechnol. Prog.* 18 (3) (2002) 623–628, <https://doi.org/10.1021/bp020028h>.
- Young Sun Jeong, Sunwha Cho, Jung Sun Park, Yong Ko, Yong-Kook Kang, Phosphorylation of Serine-10 of Histone H3 shields modified Lysine-9 selectively during mitosis, *Genes Cells* 15 (3) (2010) 181–192, <https://doi.org/10.1111/j.1365-2443.2009.01375.x>.
- Norman A. Johnson, Hybrid incompatibility genes: Remnants of a genomic battlefield? *Trends Genet.* 26 (7) (2010) 317–325, <https://doi.org/10.1016/j.tig.2010.04.005>.
- Pavan Kumar Kakumani, Pawan Malhotra, Sunil K. Mukherjee, Raj K. Bhatnagar, A draft genome assembly of the army worm, *Spodoptera frugiperda*, *Genomics* 104 (2) (2014) 134–143, <https://doi.org/10.1016/j.ygeno.2014.06.005>.
- Oliver Keller, Florian Odronitz, Mario Stanke, Martin Kollmar, Stephan Waack, Scipio: using protein sequences to determine the precise exon/intron structures of genes and their orthologs in closely related species, *BMC Bioinformatics* 9 (juin) (2008) 278, <https://doi.org/10.1186/1471-2105-9-278>.
- Peter V. Kharchenko, Artyom A. Alekseyenko, Yuri B. Schwartz, Aki Minoda, Nicole C. Riddle, Jason Ernst, Peter J. Sabo, et al., Comprehensive analysis of the chromatin landscape in *drosophila melanogaster*, *Nature* 471 (7339) (2011) 480–485, <https://doi.org/10.1038/nature09725>.
- Mikhail S. Klenov, Sergey A. Lavrov, Anastasia D. Stolyarenko, Sergey S. Ryazansky, Alexei A. Aravin, Thomas Tuschl, Vladimir A. Gvozdev, Repeat-associated siRNAs cause chromatin silencing of retrotransposons in the *Drosophila melanogaster* germline, *Nucleic Acids Res.* 35 (16) (2007) 5430–5438, <https://doi.org/10.1093/nar/gkm576>.
- Yutaka Kondo, Lanlan Shen, Saira Ahmed, Yanis Boumber, Yoshitaka Sekido, Bassem R. Haddad, Jean-Pierre J. Issa, Downregulation of histone H3 lysine 9 methyltransferase G9a induces centrosome disruption and chromosome instability in cancer cells, *PLoS One* 3 (4) (2008), <https://doi.org/10.1371/journal.pone.0002037>.
- Monika Lachner, Dónal O'Carroll, Stephen Rea, Karl Mechtler, Thomas Jenwein, Methylation of histone H3 Lysine 9 creates a binding site for HP1 proteins, *Nature* 410 (6824) (2001) 116–120, <https://doi.org/10.1038/35065132>.
- Ben Langmead, Cole Trapnell, Mihai Pop, Steven L. Salzberg, Ultrafast and memory-efficient alignment of short DNA sequences to the human genome, *Genome Biol.* 10 (3) (2009) R25, <https://doi.org/10.1186/gb-2009-10-3-r25>.

- [39] Le Thomas, Alicia K. Adrien, Alexandre Webster Rogers, Georgi K. Marinov, Susan E. Liao, Edward M. Perkins, Junho K. Hur, Alexei A. Aravin, Katalin Fejes Tóth, Piwi Induces PiRNA-guided transcriptional silencing and establishment of a repressive chromatin state, *Genes Dev.* 27 (4) (2013) 390–399, <https://doi.org/10.1101/gad.209841.112>.
- [40] Yuh Chwen G. Lee, Yuki Ogiyama, Nuno M.C. Martins, Brian J. Beliveau, David Acevedo, C. Ting Wu, Giacomo Cavalli, Gary H. Karpen, Pericentromeric heterochromatin is hierarchically organized and spatially contacts H3K9me2 Islands in euchromatin, *PLoS Genet.* 16 (3) (2020) e1008673, <https://doi.org/10.1371/journal.pgen.1008673>.
- [41] Fabrice Legeai, Sylvie Gimenez, Bernard Duvic, Jean-Michel Escoubas, Anne-Sophie Gosselin Grenet, Florence Blanc, François Cousserans, et al., Establishment and analysis of a reference transcriptome for *Spodoptera frugiperda*, *BMC Genomics* 15 (aout) (2014) 704, <https://doi.org/10.1186/1471-2164-15-704>.
- [42] Heng Li, Bob Handsaker, Alec Wysoker, Tim Fennell, Jue Ruan, Nils Homer, Gabor Marth, Goncalo Abecasis, Richard Durbin, 1000 Genome Project Data Processing Subgroup, The sequence alignment/Map format and SAMtools, *Bioinformatics* 25 (16) (2009) 2078–2079, <https://doi.org/10.1093/bioinformatics/btp352>.
- [43] Hongmei Li-Baylary, Li Yang, Hume Stroud, Suhua Feng, Thomas C. Newman, Megan Kaneda, Kirk K. Hou, et al., RNA interference knockdown of DNA methyltransferase 3 affects gene alternative splicing in the honey bee, *Proc. Natl. Acad. Sci.* 110 (31) (2013) 12750–12755, <https://doi.org/10.1073/pnas.1310735110>.
- [44] Tao Liu, Andreas Rechtsteiner, Thea A. Egelhofer, Anne Vielle, Isabel Latorre, Ming-Sin Cheung, Sevinc Ercan, et al., Broad chromosomal domains of histone modification patterns in *C. elegans*, *Genome Res.* 21 (2) (2011) 227–236, <https://doi.org/10.1101/gr.115519.110>.
- [45] Gwen Lomber, Lori Wallrath, Raul Urrutia, The heterochromatin protein 1 family, *Genome Biol.* 7 (7) (2006) 228, <https://doi.org/10.1186/gb-2006-7-7-228>.
- [46] K. Luger, A.W. Mäder, R.K. Richmond, D.F. Sargent, T.J. Richmond, Crystal structure of the nucleosome core particle at 2.8 Å resolution, *Nature* 389 (6648) (1997) 251–260, <https://doi.org/10.1038/38444>.
- [47] Madani Tonekaboni, Seyed Ali, Benjamin Haibe-Kains, Mathieu Lupien, Large organized chromatin lysine domains help distinguish primitive from differentiated cell populations, *Nat. Commun.* 12 (1) (2021) 499, <https://doi.org/10.1038/s41467-020-20830-9>.
- [48] Christèle Maison, Geneviève Almouzni, HP1 and the dynamics of heterochromatin maintenance, *Nat. Rev. Mol. Cell Biol.* 5 (4) (2004) 296–304, <https://doi.org/10.1038/nrm1355>.
- [49] Holocentromeres in rhynchospora are associated with genome-wide centromere-specific repeat arrays interspersed among euchromatin, in: André Marques, Tiago Ribeiro, Pavel Neumann, Jiri Macas, Petr Novák, Veit Schubert, Marco Pellino (Eds.), *Proceedings of the National Academy of Sciences* vol. 112 (44), 2015, pp. 13633–13638, <https://doi.org/10.1073/pnas.1512255112>.
- [50] Daniël P. Melters, Keith R. Bradnam, Hugh A. Young, Natalie Telis, Michael R. May, J. Graham Ruby, Robert Sebra, et al., Comparative analysis of tandem repeats from hundreds of species reveals unique insights into centromere evolution, *Genome Biol.* 14 (1) (2013) R10, <https://doi.org/10.1186/gb-2013-14-1-r10>.
- [51] Daniël P. Melters, Leocadia V. Paliulis, Ian F. Korf, Simon W.L. Chan, Holocentric chromosomes: convergent evolution, meiotic adaptations, and genomic analysis, *Chromosome Res.* 20 (5) (2012) 579–593, <https://doi.org/10.1007/s10577-012-9292-1>.
- [52] E. Minc, Y. Allory, H.J. Worman, J.C. Courvalin, B. Buendia, Localization and phosphorylation of HP1 proteins during the cell cycle in mammalian cells, *Chromosoma* 108 (4) (1999) 220–234, <https://doi.org/10.1007/s004120050372>.
- [53] H. Mitsunobu, M. Izumi, H. Mon, T. Tatsuke, J.M. Lee, T. Kusakabe, Molecular characterization of heterochromatin proteins 1a and 1b from the silkworm, *Bombix mori*, *Insect Mol. Biol.* 21 (1) (2012) 9–20, <https://doi.org/10.1111/j.1365-2583.2011.01115.x>.
- [54] Yves Moné, Sandra Nhim, Sylvie Gimenez, Fabrice Legeai, Imène Seninet, Hugues Parrinello, Nicolas Nègre, Emmanuelle d'Alençon, Characterization and expression profiling of microRNAs in response to plant feeding in two host-plant strains of the lepidopteran pest *Spodoptera frugiperda*, *BMC Genomics* 19 (1) (2018) 804, <https://doi.org/10.1186/s12864-018-5119-6>.
- [55] Kiwoong Nam, Sandra Nhim, Stéphanie Robin, Anthony Bretaudeau, Nicolas Nègre, Emmanuelle d'Alençon, Divergent selection causes whole genome differentiation without physical linkage among the targets in *Spodoptera frugiperda* (Noctuidae), *bioRxiv* (2018), <https://doi.org/10.1101/452870>, 452870.
- [56] Kiwoong Nam, Sandra Nhim, Stéphanie Robin, Anthony Bretaudeau, Nicolas Nègre, Emmanuelle d'Alençon, Positive selection alone is sufficient for whole genome differentiation at the early stage of speciation process in the fall armyworm, *BMC Evol. Biol.* 20 (1) (2020) 152, <https://doi.org/10.1186/s12862-020-01715-3>.
- [57] Subhiksha Nandakumar, Hailun Ma, Arifa S. Khan, Whole-genome sequence of the *Spodoptera frugiperda* Sf9 insect cell line, *Genome Announc.* 5 (34) (2017), <https://doi.org/10.1128/genomeA.00829-17>.
- [58] Nicolas Nègre, Sergey Lavrov, Jérôme Hennequin, Michel Bellis, Giacomo Cavalli, Mapping the distribution of chromatin proteins by ChIP on chip, in: *Methods in Enzymology* 410, Academic Press, 2006, pp. 316–341, [https://doi.org/10.1016/S0076-6879\(06\)10015-4](https://doi.org/10.1016/S0076-6879(06)10015-4). DNA Microarrays, Part A: Array Platforms and Wet-Bench Protocols.
- [59] Petr Nguyen, Ken Sahara, Atsuo Yoshido, Frantisek Marec, Evolutionary dynamics of rDNA clusters on chromosomes of moths and butterflies (Lepidoptera), *Genetica* 138 (3) (2010) 343–354, <https://doi.org/10.1007/s10709-009-9424-5>.
- [60] Petr Novák, Pavel Neumann, Jiri Pech, Jaroslav Steinhaisl, Jiri Macas, RepeatExplorer: A galaxy-based web server for genome-wide characterization of Eukaryotic repetitive elements from next-generation sequence reads, *Bioinformatics* (Oxford, England) vol. 29 (6) (2013) 792–793, <https://doi.org/10.1093/bioinformatics/btt054>.
- [61] Ludmila Oliveira, Pavel Neumann, Tae-Soo Jang, Sonja Klemme, Veit Schubert, Andrea Koblikova, Andreas Houben, Jiri Macas, Mitotic spindle attachment to the holocentric chromosomes of *Cuscuta Europaea* does not correlate with the distribution of CENH3 chromatin, *Front. Plant Sci.* 10 (2020), <https://doi.org/10.3389/fpls.2019.01799>.
- [62] Marion Orsucci, Yves Moné, Philippe Audiot, Sylvie Gimenez, Sandra Nhim, Rima Naït-Saïdi, Marie Frayssinet, et al., Transcriptional differences between the two host strains of *Spodoptera frugiperda* (Lepidoptera: Noctuidae), *BioRxiv* (2020) 263186, <https://doi.org/10.1101/263186>, juin.
- [63] Mihaela Pertea, Geo M. Pertea, Corina M. Antonescu, Tsung-Cheng Chang, Joshua T. Mendell, Steven L. Salzberg, StringTie enables improved reconstruction of a transcriptome from RNA-Seq reads, *Nat. Biotechnol.* 33 (3) (2015) 290–295, <https://doi.org/10.1038/nbt.3122>.
- [64] Andrey Poleshko, Cheryl L. Smith, Son C. Nguyen, Priya Sivaramakrishnan, Karen G. Wong, John Isaac Murray, Melike Lakadamyali, Eric F. Joyce, Rajan Jain, Jonathan A. Epstein, H3K9me2 orchestrates inheritance of spatial positioning of peripheral heterochromatin through mitosis. Ed. Andrés Aguilera, Jessica K Tyler, and Andrew S Belmont, *eLife* 8 (octobre) (2019), <https://doi.org/10.7554/eLife.49278> e49278.
- [65] Christophe Rachez, Rachel Legendre, Mickaël Costallat, Hugo Varet, Jia Yi, Etienne Kornobis, Caroline Proux, Christian Muchardt, An impact of HP1γ on the fidelity of pre-mRNA splicing arises from its ability to bind RNA via intronic repeated sequences, *BioRxiv* (2019) 686790, <https://doi.org/10.1101/686790>, juin.
- [66] Fidel Ramírez, Devon P. Ryan, Björn Grüning, Vivek Bhardwaj, Fabian Kilpert, Andreas S. Richter, Steffen Heyne, Friederike Dündar, Thomas Manke, DeepTools2: A next generation web server for deep-sequencing data analysis, *Nucleic Acids Res.* 44 (W1) (2016) W160–W165, <https://doi.org/10.1093/nar/gkw257>.
- [67] S. Rea, F. Eisenhaber, D. O'Carroll, B.D. Strahl, Z.W. Sun, M. Schmid, S. Opravil, et al., Regulation of chromatin structure by site-specific histone H3 methyltransferases, *Nature* 406 (6796) (2000) 593–599, <https://doi.org/10.1038/35020506>.
- [68] Nicole C. Riddle, Aki Minoda, Peter V. Kharchenko, Artymov A. Alekseyenko, Yuri B. Schwartz, Michael Y. Tolstorukov, Andrey A. Gorchakov, et al., Plasticity in patterns of histone modifications and chromosomal proteins in *Drosophila* heterochromatin, *Genome Res.* 21 (2) (2011) 147–163, <https://doi.org/10.1101/gr.110098.110>.
- [69] Robinson, *Lepidoptera Genetics* 1971, 1971. <https://www.elsevier.com/books/lepidoptera-genetics/robinson/978-0-08-006659-2>.
- [70] Parna Saha, Divya Tej Sowpati, Mamilla Soujanya, Ishanee Srivastava, Rakesh Kumar Mishra, Interplay of pericentromeric genome organization and chromatin landscape regulates the expression of *Drosophila melanogaster* heterochromatic genes, *Epigenetics Chromatin* 13 (1) (2020) 41, <https://doi.org/10.1186/s13072-020-00358-4>.
- [71] Violaine Saint-André, Eric Batsché, Christophe Rachez, Christian Muchardt, Histone H3 Lysine 9 trimethylation and HP1γ favor inclusion of alternative exons, *Nat. Struct. Mol. Biol.* 18 (3) (2011) 337–344, <https://doi.org/10.1038/nsmb.1995>.
- [72] P.R.V. Satyaki, Tawny N. Cuykendall, Kevin H.-C. Wei, Nicholas J. Brideau, S. Hojoong Kwak, Patrick M. Aruna, Shuqing Ji Ferree, Daniel A. Barbash, The Hmr and Lhr hybrid incompatibility genes suppress a broad range of heterochromatic repeats, *PLoS Genet.* 10 (3) (2014), e1004240, <https://doi.org/10.1371/journal.pgen.1004240>.
- [73] Stefan Schoeftner, Maria A. Blasco, Chromatin regulation and non-coding RNAs at mammalian telomeres, *Semin. Cell Dev. Biol.* 21 (2) (2010) 186–193, <https://doi.org/10.1016/j.semdev.2009.09.015>.
- [74] Franz Schrader, Notes on the mitotic behavior of long chromosomes, *Cytologia* 6 (4) (1935) 422–430, <https://doi.org/10.1508/cytologia.6.422>.
- [75] Aruni P. Senaratne, Héloïse Muller, Kelsey A. Fryer, Munetaka Kawamoto, Susumu Katsuma, Ines A. Drinnenberg, Formation of the CenH3-deficient holocentromere in lepidoptera avoids active chromatin, *Curr. Biol.* 31 (1) (2021) 173–181.e7, <https://doi.org/10.1016/j.cub.2020.09.078>.
- [76] Peter J. Shaw, Peter C. McKeown, The structure of rDNA chromatin, in: Mark O. J. Olson (Ed.), *The Nucleolus*, Springer, New York, NY, 2011, pp. 43–55, https://doi.org/10.1007/978-1-4614-0514-6_3. Protein Reviews.
- [77] Grzegorz Sienski, Derya Dönertas, Julius Brennecke, Transcriptional silencing of transposons by piwi and maelstrom and its impact on chromatin state and gene expression, *Cell* 151 (5) (2012) 964–980, <https://doi.org/10.1016/j.cell.2012.10.040>.
- [78] Daniel F. Simola, Riley J. Graham, Cristina M. Brady, Brittany L. Enzmann, Claude Desplan, Anandasankar Ray, Laurence J. Zwiebel, et al., Epigenetic (Re) programming of caste-specific behavior in the ant *Camponotus floridanus*, *Science* (New York, N.Y.) vol. 351 (6268) (2016) aac6633, <https://doi.org/10.1126/science.aac6633>.
- [79] Rakesh Srivastava, Rashmi Srivastava, Seong Hoon Ahn, The epigenetic pathways to ribosomal DNA silencing, *Microbiol. Mol. Biol. Rev.* 80 (3) (2016) 545–563, <https://doi.org/10.1128/MMBR.00005-16>.
- [80] Slavica Stanojic, Sylvie Gimenez, Emmanuelle Permal, François Cousserans, Hadi Quesneville, Philippe Fournier, Emmanuelle d'Alençon, Correlation of LNCr RasiRNAs expression with heterochromatin formation during development of the

- holocentric insect Spodoptera frugiperda, PLoS One 6 (9) (2011), <https://doi.org/10.1371/journal.pone.0024746>.
- [81] Florian A. Steiner, Steven Henikoff, Holocentromeres are dispersed point centromeres localized at transcription factor hotspots, Ed. Asifa Akhtar, eLife 3 (avril) (2014), e02025, <https://doi.org/10.7554/eLife.02025>.
- [82] Juan A. Subirana, Xavier Messegue, A satellite explosion in the genome of holocentric nematodes, PLoS One 8 (4) (2013), <https://doi.org/10.1371/journal.pone.0062221>.
- [83] Beth A. Sullivan, Gary H. Karpen, Centromeric chromatin exhibits a histone modification pattern that is distinct from both euchromatin and heterochromatin, Nat. Struct. Mol. Biol. 11 (11) (2004) 1076–1083, <https://doi.org/10.1038/nsmb845>.
- [84] M. Tachibana, K. Sugimoto, T. Fukushima, Y. Shinkai, Set domain-containing protein, G9a, is a novel lysine-preferring mammalian histone methyltransferase with hyperactivity and specific selectivity to lysines 9 and 27 of histone H3, J. Biol. Chem. 276 (27) (2001) 25309–25317, <https://doi.org/10.1074/jbc.M101914200>.
- [85] Makoto Tachibana, Kenji Sugimoto, Masami Nozaki, Jun Ueda, Tsutomu Ohta, Misao Ohki, Mikiko Fukuda, et al., G9a histone methyltransferase plays a dominant role in euchromatic histone H3 lysine 9 methylation and is essential for early embryogenesis, Genes Dev. 16 (14) (2002) 1779–1791, <https://doi.org/10.1101/gad.989402>.
- [86] Denis Tagu, John K. Colbourne, Nicolas Nègre, Genomic data integration for ecological and evolutionary traits in non-model organisms, BMC Genomics 15 (1) (2014) 490, <https://doi.org/10.1186/1471-2164-15-490>.
- [87] Helga Thorvaldsdóttir, James T. Robinson, Jill P. Mesirov, Integrative Genomics Viewer (IGV): high-performance genomics data visualization and exploration, Brief. Bioinform. 14 (2) (2013) 178–192, <https://doi.org/10.1093/bib/bbs017>.
- [88] J.L. Vaughn, R.H. Goodwin, G.J. Tompkins, P. McCawley, The establishment of two cell lines from the insect spodoptera frugiperda (Lepidoptera; Noctuidae), In Vitro 13 (4) (1977) 213–217, <https://doi.org/10.1007/BF02615077>.
- [89] Pernette J. Verschure, Ineke van der Kraan, Wim de Leeuw, Johan van der Vlag, Anne E. Carpenter, Andrew S. Belmont, Roel van Driel, In vivo HP1 targeting causes large-scale chromatin condensation and enhanced histone lysine methylation, Mol. Cell. Biol. 25 (11) (2005) 4552–4564, <https://doi.org/10.1128/MCB.25.11.4552-4564.2005>.
- [90] Alisa O. Vershinina, Boris A. Anokhin, Vladimir A. Lukhtanov, « Ribosomal DNA clusters and telomeric (TTAGG)_n repeats in blue butterflies (Lepidoptera, Lycaenidae) with low and high chromosome numbers ». Comparative, Cytogenetics 9 (2) (2015) 161–171, <https://doi.org/10.3897/CompCytogen.v9i2.4715>.
- [91] L.L. Wallrath, S.C. Elgin, Position effect variegation in drosophila is associated with an altered chromatin structure, Genes Dev. 9 (10) (1995) 1263–1277, <https://doi.org/10.1101/gad.9.10.1263>.
- [92] Bo Wen, Wu Hao, Yoichi Shinkai, Rafael A. Irizarry, Andrew P. Feinberg, Large organized chromatin K9-modifications (LOCKS) distinguish differentiated from embryonic stem cells, Nat. Genet. 41 (2) (2009) 246–250, <https://doi.org/10.1038/ng.297>.
- [93] Klaus Werner Wolf, The structure of condensed chromosomes in mitosis and meiosis of insects, Int. J. Insect Morphol. Embryol. 25 (1) (1996) 37–62, [https://doi.org/10.1016/0020-7322\(95\)00021-6](https://doi.org/10.1016/0020-7322(95)00021-6).
- [94] Jiro C. Yasuhara, Barbara T. Wakimoto, Molecular landscape of modified histones in drosophila heterochromatic genes and euchromatin-heterochromatin transition zones, PLoS Genet. 4 (1) (2008), e16, <https://doi.org/10.1371/journal.pgen.0040016>.
- [95] František Zedek, Petr Bureš, Absence of positive selection on CenH3 in Luzula suggests that holokinetic chromosomes may suppress centromere drive, Ann. Bot. 118 (7) (2016) 1347–1352, <https://doi.org/10.1093/aob/mcw186>.
- [96] Lei Zhang, Bo Liu, Weigang Zheng, Conghui Liu, Dandan Zhang, Shengyuan Zhao, Zaiyuan Li, et al., Genetic structure and insecticide resistance characteristics of fall armyworm populations invading China, Mol. Ecol. Resour. 20 (6) (2020) 1682–1696, <https://doi.org/10.1111/1755-0998.13219>.
- [97] Yong Zhang, Tao Liu, Clifford A. Meyer, Jérôme Eeckhoutte, David S. Johnson, Bradley E. Bernstein, Chad Nusbaum, et al., Model-based analysis of ChIP-Seq (MACS), Genome Biol. 9 (9) (2008) R137, <https://doi.org/10.1186/gb-2008-9-9-r137>.
- [98] H. Quesneville, C.M. Bergman, O. Andrieu, D. Autard, D. Nouaud, et al., Combined evidence annotation of transposable elements in genome sequences, PLoS Comput. Biol. 1 (2) (2005) e22, <https://doi.org/10.1371/journal.pcbi.0010022>.